



Dose-effect calibration curve for high X-ray doses using the Calyculin-A chromosome premature condensation assay

Chaves-Campos, F.A.^{a,b,c,d*}; Ortíz-Morales, F.^{a,d}; Mejías-Gamboa, R.^a;
González-Mesa, J.E.^{d,e}; García-Lima, O.^{d,e}; Rodríguez-Valerio, M.P.^b;
Vargas-Segura, W.^{f,g}; Cordero-Ramírez, A.^{f,h}.

^aHealth Research Institute (INISA), University of Costa Rica. San José, Costa Rica.

^bSchool of Health Technologies, University of Costa Rica. San José, Costa Rica.

^cRobotic Radiosurgery Center, San José Costa Rica.

^dLatin American Biological Dosimetry Network (LBDNet).

^eCentro de Protección e Higiene de las Radiaciones (CPHR), Habana, Cuba.

^fRadiotherapy Department. Hospital México. Costa Rican Social Security

^gPhysics Department. Costa Rican Institute of Technology, ITCR. Cartago, Costa Rica.

^hResearch Center in Materials Science and Engineering (CICIMA), University of Costa Rica, San José, Costa Rica

*Correspondence: fabio.chavescampos@ucr.ac.cr

Abstract: Purpose: This article shows the results of the Cytogenetics Laboratory of the Health Research Institute (INISA) to develop a dose-effect calibration curve with the Calyculin-A chemical induction premature condensation assay to estimate high doses of X-ray exposure. Methods: to create the calibration curve, peripheral blood samples from two participants (one female and one male) were exposed to X-rays at six different dose points ranging from 0 to 17.5 Gy in vitro. The irradiated blood was cultured for 48 hours according to international protocols, and the resulting chromosome rings were recorded. We used BioDoseTools software to calculate the coefficients for the calibration curve. Results: The coefficients of the curve are $\alpha: 0.028 \pm 0.001$ and $C: 0.001 \pm 0.001$. These coefficients have similar values to those reported internationally. The curve was validated by calculating an unknown dose exposed to 6 Gy; the estimated dose was 5.651 ± 0.636 Gy, with no statistically significant differences between the dose delivered and the estimated dose. Conclusions: The INISA Biological Dosimetry Service can use the curve obtained to assess absorbed doses in cases of suspected overexposure to high X-ray doses.

Keywords: biodosimetry, cytogenetic aberrations, Calyculin-A, radiation protection, radiation biology.



Curva de calibración dosis-efecto para altas dosis de rayos X utilizando el ensayo de condensación prematura de cromosomas con Caliculina-A

Resumen: Propósito: este artículo muestra los resultados del Laboratorio de Citogenética del Instituto de Investigación Sanitaria (INISA) para desarrollar una curva de calibración dosis-efecto con el ensayo de condensación prematura por inducción química de caliculina-A para estimar altas dosis de exposición a rayos X. Métodos: para crear la curva de calibración, se expusieron muestras de sangre periférica *in vitro* de dos participantes (una mujer y un hombre) en seis puntos de dosis diferentes que oscilaban entre 0 y 17,5 Gy de rayos X. La sangre irradiada se cultivó durante 48 horas según los protocolos internacionales y se registraron los anillos cromosómicos resultantes. Se utilizó el programa BioDoseTools para calcular los coeficientes de la curva de calibración. Resultados: Los coeficientes de la curva son α $0,028 \pm 0,001$ y C: $0,001 \pm 0,001$. Estos coeficientes tienen valores similares a los reportados internacionalmente. La curva se validó calculando una dosis desconocida expuesta a 6 Gy; la dosis estimada fue de $5,651 \pm 0,636$ Gy, sin diferencias estadísticamente significativas entre la dosis administrada y la dosis estimada. Conclusiones: El Servicio de Dosimetría Biológica del INISA puede utilizar la curva obtenida para estimar dosis absorbidas en casos de sospecha de sobreexposición a altas dosis de rayos X.

Palabras clave: biodosimetría, aberraciones citogenéticas, Caliculina-A, protección radiológica, biología de las radiaciones.

1. INTRODUCTION

Having multiple dose-effect calibration curves is crucial for reliable biological dosimetry services. These curves establish the relationship between radiation doses and the frequency of a cytogenetic biomarker observed at each dose point. Various cytogenetic assays are used in biodosimetry, including the premature chromosome condensation assay (PCCr), cytokinesis-blocked micronucleus assay, Fluorescence In Situ Hybridization (FISH) chromosome translocation assay, and the dicentric chromosomes assay (DCA). The latter is considered the gold standard biodosimetric technique and the most sensitive biological method for measuring radiation exposure. This is due to the specificity of the biomarker to ionizing radiation, as only a select few genotoxic agents can induce their formation. The frequency of dicentric chromosomes increases proportionally to the administered dose, making it a reliable indicator of radiation exposure levels [1]. Estimating doses above 5 Gy using the DCA may prove challenging due to radiation-induced mitotic delay and extensive cell death. Consequently, obtaining the necessary number of cells for analysis and dose estimation may not be attainable [2, 3].

To prepare chromosomes for analysis, the DCA involves arresting cells in metaphase by adding Colcemid 2 or 3 hours before terminating the cultures. An alternative technique for obtaining chromosomes for microscopic analysis is the PCCr, which allows the visualization of interphase chromatin as condensed chromosomes. The PCCr enables the determination of the frequency of chromosomal rings caused by exposure to different doses of ionizing radiation and has proven valuable in estimating radiation doses ranging from 0.2 to 20 Gy [4].

While multiple techniques are available for premature condensation of chromosomes outside mitosis, one of the earliest methods involves the fusion of human lymphocytes with

CHO cells (Chinese hamster ovary cells). This procedure commonly utilizes polyethylene glycol as a fusion agent [5].

A revised version of the PCCr assay involves using specific serine/threonine phosphatase activity inhibitors, such as okadaic acid and Calyculin-A, to induce chemical changes in PCCr cells. Calyculin-A, originally extracted from the marine sponge species *Discodermia calyx*, inhibits serine-threonine phosphatases type 1 and 2. By deactivating these enzymes, premature chromosome condensation occurs in all phases of the cell cycle (G1, S, G2, M), allowing interphase chromatin to be viewed as mitotic chromosomes. Consequently, analysis can be conducted on both metaphase and non-metaphase chromosomes. Furthermore, peripheral lymphocytes can undergo early chromosome condensation using okadaic acid and Calyculin-A [2, 6].

The primary mechanism of chromosome ring formation by ionizing radiation involves the induction of two double-strand breaks, each occurring in the terminal regions of both arms of a single chromosome. Subsequently, these breaks are repaired and fused, resulting in a ring-shaped structure. Consequently, centromeric rings arise as a result of intrachromosomal rearrangements [7].

Additionally, the formation of rings can occur through the fusion of dysfunctional telomeres. Ionizing radiation-induced oxidative stress can lead to alterations in the structure and function of telomeres, potentially impacting their stability and functionality. These modifications may contribute to the formation of chromosome rings [8, 9].

This article highlights the Health Research Institute's (INISA) work to obtain a dose-effect calibration curve using the PCCr assay with chemical induction via Calyculin-A for dose estimation in the 0-17.5 Gy range of X-rays. A notable aspect of this biodosimetry study is the use of robotic radiosurgery equipment as the irradiation platform, coupled with the semi-automated analysis of cell images from digitized slides.

The Cytogenetics Laboratory at INISA is the first Biological Dosimetry Service in Central America. The laboratory has a dose-effect calibration curve for gamma rays, to estimate

exposures from 0 to 5 Gy. The present study shows the efforts made by the laboratory for the construction of a dose-effect curve using the PCCr assay. Additionally, the laboratory is currently working on obtaining calibration curves for X-rays using two distinct methods: the cytokinesis-block micronucleus and dicentric chromosome + caffeine assay [5, 10].

2. MATERIALS AND METHODS

2.1. Collection and irradiation of blood samples.

Six 5 mL blood samples were individually collected in heparinized Vacutainer tubes from each two participants. Subsequently, these samples underwent exposure to a 6 MeV X-ray beam using a CyberKnife® Robotic Radiosurgery system (Accuray, Sunnyvale, CA, USA) owned by the Robotic Radiosurgery Center in La Uruca, San José, Costa Rica.

The CyberKnife® was calibrated and validated according to the recommendations of the Technical Report Series No 483 (TRS 483) of the International Atomic Energy Agency [11] and the Report TG 135 of the AAPM [12]. For dose delivery, the samples were positioned at the central point of a 30 cm x 30 cm water phantom (PTW, Freiburg, Germany), with the beam exit set up perpendicularly to the faces of the phantom. The source-to-surface distance (SSD) was maintained at 65.7 cm on one side (thin window) and 65 cm on the other side.

The 6MV beam was administered using a 6 cm diameter cone at a nominal dose rate of 1000 cGy/min, with a reference distance of 80 cm. The CyberKnife® system was calibrated to deliver 1 cGy/MU at a depth of 1.5 cm in water following the aforementioned reference conditions. For each dose value, the dose calculation was divided into two radiation fields normalized to the effective central point of the phantom.

The Monitor Units (MU) required to deliver a specific dose were calculated using Equation 1 and considering the manufacturer's recommendations. Beam heterogeneity was not accounted for during MU calculations or dose analysis.

$$\text{MU} = \frac{X(\text{cGy})}{1\text{cGy/MU} \cdot (800^2/\text{SAD}^2) \cdot \text{OCR}(\text{R800, col, Deff}) \cdot \text{TPR}(\text{Deff, EFW}) \cdot \text{OF}(\text{SAD, Col})} \quad (1)$$

The factors described in the equation are:

- X: dose value.
- cGy/MU: dose rate.
- SAD: source axis distance (used in the inverse square factor).
- OCR: Off-center ratio.
- TPR: Tissue-phantom ratio.
- OF: Output Factor (for distance and collimator).

The study included six exposure doses ranging from 0 to 17.5 Gy: 0.0, 5.0, 7.5, 10, 12.5, and 17.5 Gy. An additional sample was exposed to a dose of 6 Gy, unbeknownst to the analysts. Samples were placed inside a water phantom at a temperature of $37^\circ\text{C} \pm 0.5$ and irradiated, with the irradiation fields adjusted to the dimensions of the tube to homogenize the dose.

To ensure temperature stability of blood samples post-irradiation and during transportation between centers, a portable incubator model INB-203M Portable CO₂ (IKS International) was employed. With a 15 L capacity, it facilitated safe handling and transport of samples in a controlled environment at 37°C . Following irradiation, the samples were incubated at $37 \pm 0.5^\circ\text{C}$ for approximately two hours, providing adequate time for the activation of cellular DNA damage response mechanisms.

The research protocol underwent scrutiny and received approval from the Scientific Ethical Committee of the University of Costa Rica (UCR). Before proceeding with sample collection, thorough explanations regarding donor participation and the intended utilization of the samples were provided. All personal information was anonymized, with coding procedures exclusively accessible to the principal investigator.

2.2. Premature Chromosome Condensation Assay

Lymphocyte culture, cell harvesting, preparation of cell slides, and cytogenetic analysis of ring chromosomes were performed according to the protocol described by the IAEA [5].

Initially, a volume of 0.5 mL of blood was added consecutively into two distinct conical tubes, each containing 4.5 mL of PBMax culture medium (Gibco brand) (supplemented with Phytohemagglutinin (PHA) at a concentration of 3%). The tubes were then incubated at 37°C in a 5% CO₂ atmosphere for 48 hours.

After 24 hours of starting the culture, 24 µl of Colcemid (Gibco brand) was added to each culture to achieve mitotic arrest. This addition resulted in a final concentration of 40 ng/ml. After 47 hours of starting the culture, 12 µl of Calyculin A was added and incubated for an additional hour. The final concentration of Calyculin A was 50 nM.

Cell harvesting began after 48 hours of culturing by centrifuging the cultures at 1200-1300 rpm for 10 minutes to remove the supernatant. Next, the cell button was resuspended, and 7 mL of KCl (0.075 mol/L) was added at 37°C to induce hypotonic shock. The tubes were then incubated for 35 minutes, followed by the addition of 1 mL of fixative (3:1 methanol/acetic acid solution) to each tube. After centrifuging at 1200 rpm for 10 minutes, the supernatant was discarded, and the cell button was resuspended with 1 mL of the fixative solution. Subsequently, 10 mL of fixative was added dropwise continuously while agitating. The centrifugation and fixative wash cycle were repeated two to three times until the cell button appeared whitish. Finally, the tubes were centrifuged to remove the supernatant, leaving twice as much fixative as the size of the cell button. The cells were stored in their first or subsequent fixations under refrigeration for 24-48 hours.

The cell suspension was dropped onto clean slides and air-dried for 24 hours. After drying, they were stained with Giemsa solution (50 ml H₂O, 50 ml GURR Buffer, 1 ml Giemsa), followed by rinsing with distilled water.

2.3. Microscopic analysis

The image capture process was conducted using an automated microscope, specifically the MetaSystem Metafer version 3.13.3. The analysis of images and scoring of chromosome rings scoring were carried out by skilled personnel from the INISA cytogenetics laboratory, making the overall process semi-automated.

The MetaArchive 5.4 software recorded the analyzed cells and the aberrations detected. Afterward, an Excel 2016 spreadsheet was prepared to show the number of cells analyzed per dose point, the total number of rings, and the number of rings per cell. This data was used to determine the frequency of aberrations at each dose point and their distribution.

2.4. Analysis criteria for the PCCr assay and for scoring chromosome ring frequencies

For each dose, a minimum of 1000 cells were analyzed. Ring frequencies were documented solely for cells in the G1, G2, metaphase, and anaphase phases. The morphology of chromosomes in PCCr cells varies depending on the phase of the cell cycle when premature condensation is induced: [13], [14]

- G1: Characterized by univalent chromosomes (unduplicated DNA, single chromatid).
- S: Characterized by a combination of single-stranded and double-stranded chromosomes with a shattered appearance.
- G2: Characterized by bivalent chromosomes (duplicated DNA, presence of two joined chromatids) with no defined centromere.
- Metaphase: Characterized by bivalent chromosomes (duplicated DNA, presence of two united chromatids) with a defined centromere.
- Anaphase: Characterized by separate chromatids forming an angle from the centromere with a defined centromere.

There are two distinct types of chromosome rings: solid and hollow. Solid chromosome rings lack openings or hollow spaces, while their hollow counterparts feature an opening or hollow space at the center. Hollow chromosome rings can possess diverse configurations due to chromosome cross-linking and can vary in size. Solid rings are usually round and small; to be considered as such, their diameter must be larger than the width of the chromatids of the chromosomes in that cell.

For the scoring of rings, the following criteria were considered [14]:

- When DNA duplication was not observed, each ring was treated as an independent entity.
- In cells with duplicated DNA, only one ring was recorded under the following conditions:
 - If two separate rings of equal size were observed.
 - If two intertwined rings were observed.
 - If a single chromatid ring was observed.
 - Each double chromatid ring was recorded as a separate entity, irrespective of size.

2.5. Statistical analysis

The statistical data processing for this study was conducted using the BioDose Tools application [15]. This included calibration curve fitting, estimation of unknown doses, calculation of dispersion statistics for calibration fit, and graphical analysis. The chi-square goodness-of-fit statistic and Student's t-test were utilized to assess the statistical significance of estimated coefficients. For the unknown dose, the criterion for acceptance was that the estimated dose by biological dosimetry should not deviate by more than 20% from the dose determined by physical dosimetry [16-18].

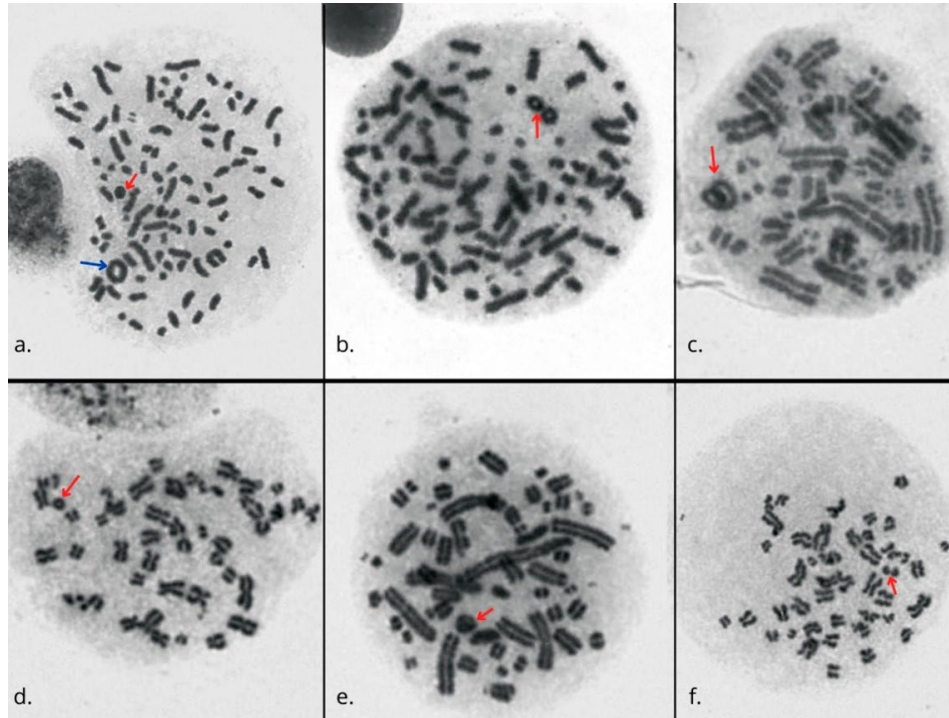
3. RESULTS AND DISCUSSION

Automated pattern recognition systems for cell identification have been successfully implemented in various laboratories, with several commercially available systems now accessible. These systems enable the digitization of whole cell slides and the creation of images for visualization and analysis, thereby streamlining the identification and localization of aberrant chromosomes. This technological advancement expedites biodosimetry assessments and ensures consistent and reliable results. To date, there is limited documentation on the application of automated microscopy for acquiring images from preparations generated by the PCCr assay and for constructing a biodosimetric calibration curve. Moreover, studies investigating the dose-effect relationship for X-rays within this context are notably scarce.

The following images (Figure 1), assessed based on the described evaluative framework and obtained through the employment of the Metafer system, illustrate examples of chromosome rings induced by ionizing radiation within the dosage range of 0 to 17.5 Gy.

The data presented in Table 1 depicts the frequency of chromosome aberrations at different levels of irradiation doses, accompanied by the respective cell cycle stage distribution and the observed number of chromosome rings. The experimental results reveal an increase in the ring frequency with higher X-ray doses. Analysis of the aberration distribution suggests that most irradiated samples adhere to the Poisson distribution, as expected for a homogeneous scenario. The number of observed rings per cell ranges from 0 to 4, with cells exhibiting multiple damage of 2 rings becoming more prevalent from the 5 Gy dose onwards. Notably, cells with four rings were solely observed in blood samples exposed to 17.5 Gy.

Figure 1: Diverse images acquired at 63x magnification show chromosome rings in different cell cycle phases.



Source: INISA, 2023. 1a: Depicts a cell in the G2 phase presenting one solid ring (indicated by the red arrow) and one hollow ring (indicated by the blue arrow), both considered separate rings. 1b: Illustrates a cell in the G2 phase with two small hollow rings of equal size (indicated by the red arrow); however, since both rings originate from a single chromosome, only one chromosome ring is considered. 1c: Shows a cell in the G2-M phase exhibiting a hollow ring, also known as a Moebius ring, due to its configuration. 1d and 1e: Depicts metaphase cells with one small hollow ring (indicated by the red arrow) and one medium-sized hollow ring (indicated by the red arrow), respectively. 1f: Demonstrates a metaphase cell with two small hollow rings (indicated by the red arrow); only one chromosome ring is considered for scoring.

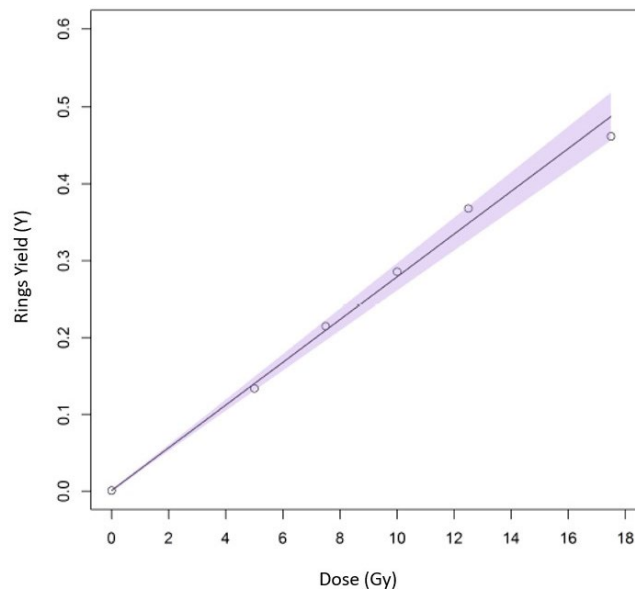
Table 1: Frequency of chromosome rings per X-ray dose

Dose	Number of analyzed cells	Cells analyzed according to cell cycle phase				Ring Chrs.	Freq.	Cell distribution according to the number of chromosome rings					DI	U
		G1	G2	M	A			0	1	2	3	4		
0	1000	2	64	910	24	1	0.00100	999	1	0	0	0	1	
5	1000	93	385	495	27	134	0.13400	882	103	14	1	0	1.1209	2.7111
7.5	1000	20	429	547	4	215	0.21500	813	163	20	4	0	1.0838	1.8763
10	1000	56	500	431	13	286	0.28600	759	202	33	6	0	1.0717	1.6056
12.5	1000	7	324	658	11	368	0.36800	697	245	51	7	0	1.0243	0.5445
17.5	1000	21	462	517	0	462	0.46200	632	287	70	9	2	1.0109	0.2433

DI: dispersion index. U: Papworth's U test. Chrs: chromosomes. Freq.: Frequency

Using the data collected, a dose-response curve was generated for human lymphocytes exposed to X-rays through the PCCr assay (Figure 2). The curve was created using 6000 analyzed cells for the 6 data points (0, 5, 7.5, 10, 12.5, and 17.5 Gy). The chromosome ring frequency (Y) exhibited a linear relationship to the delivered dose (D).

Figure 2: Dose-response curve for chromosomal rings at different X-ray doses (circle dots) with 95% confidence limits (shaded area) using the premature chromosome condensation assay in human lymphocytes.



Source: INISA, 2023.

The resulting equation from this analysis is as follows:

$$Y = (0.001 \pm 0.001) + D \times (0.028 \pm 0.001)$$

A calculated value of ' α ' was determined to be 0.028 ± 0.001 . The chi-squared tests for homogeneity were performed to compare the frequency of aberrations obtained at a given dose among different donors, but no significant differences were found. Hence, the dose-response curve was established using combined data from both donors. The p-value for goodness-of-fit was 0.5577, with $\chi^2 = 3.0008$, degrees of freedom=4. Correlation coefficient, $r^2 = 0.9960$. Table 2 shows the estimated coefficients of the calibration curve with standard errors (SE).

Table 2: Estimated coefficients of the calibration curve with standard errors

C+SE	α+SE	χ^2	DF	r^2
0.001±0.001	0.028±0.001	3.0008	4	0.9960

SE: standard error. DF: degrees of freedom.

Even with advancements in techniques and the widespread adoption of standardized statistical programs for data analysis, variations persist in calibration curves across different laboratories. Relying on a calibration curve generated elsewhere for dose interpretation introduces additional uncertainty. Consequently, it is strongly advised that any laboratory undertaking biological dosimetry takes the initiative to establish its dose-response curves [5]. Numerous laboratory reports have been published regarding the calibration. Examples of α and C coefficients for PCCr dose-response curves are shown in Table 3. As anticipated, variations in laboratory methods, including differences in blood donors, cell cultures, slide preparation, and scoring criteria, result in distinct values for the α and C coefficients. Research findings suggest that when using Calyculin-A, different treatment durations alter the morphology and size of chromosomes, impacting the yield of cells with analytical quality [19].

This suggests possible variations in the scoring of chromosome rings across the studies detailed in Table 3, introducing the possibility of influencing the observed yield in the high-dose range and potentially explaining the variations of the coefficients derived from the curve-fitting procedure. Despite the different relative biological effects associated with each low and high linear energy transfer (LET) radiation, in conjunction with variations in radiation quality, a discernible lack of differentiation becomes evident when scrutinizing coefficients for X-rays, gamma rays, neutrons, and alpha particles obtained through the PCCr assay. This characteristic sets the PCCr assay apart, particularly when juxtaposed with the DCA. In contrast to the PCCr assay, the DCA reveals noticeable differences in dose-response across various radiation types [20].

Observing discrepancies from one study to another underscores the importance of establishing the dose-response curve under the same experimental conditions as the initial dose estimation. This approach helps mitigate variations in dose estimation [21].

Table 3: Dose-response coefficients of ring chromosomes in various PCCr studies.

Reference	Mitotic inducer	Radiation Source	Energy	Doses (Gy)	C±SE	α±SE
Present Study	Cal-A	LINAC	6 MV*	0, 5, 7.5, 10, 12, 17.5	0.0010 ± 0.0010	0.0278 ± 0.0007
[22]	Cal-A	LINAC	6 MV*	0, 2, 4, 6, 8, 10, 12.5, 15, 17.5, 20	-0.03	0.049 ± 0.002
[23]	Cal-A	Co-60	1.25 MeV**	0, 5, 7.5, 10, 20, 25	0.0005 ± 0.0005	0.021 ± 0.0007
[24]	Cal-A	Cs-137	0.662 MeV*	0,0.5,1,3,5,7,10,15,20	NR	0.027 ± 0.003
[25]	Cal-A	Co-60	1.25 MeV**	0, 1, 5, 7.5, 10, 20	0.0015±0.0003	0.044 ± 0.0012
[26]	Cal-A	Co-60	1.25 MeV**	0, 1, 5, 7.5, 10, 20	0.0006 ± 0.0002	0.0303 ± 0.0008
[27]	Cal-A	Co-60	1.25 MeV**	0, 2.5, 5, 10, 15, 20	0.0001 ± 0.0001	0.0499 ± 0.0028
[4]	Cal-A	Co-60	1.25 MeV**	0, 5, 7.5, 10, 12, 17.5, 20	NR	0.0308 ± 0.0012
[28]	OA	Co-60	1.25 MeV**	0, 6.2, 12.5, 18.4, 24.5	NR	0.054 ± 0.001
[29]	OA	Co-60	1.25 MeV**	0, 1, 2.5, 5, 10, 15, 20	0.0018±0.0001	0.049 ± 0.001
[3]	OA	Co-60	1.25 MeV**	0, 2.5, 5,7.5, 10, 15, 20	NR	0.048 ± 0.002
[23]	Cal-A	fission neutrons	0.49 MeV**	0, 5.4, 5.6, 9.4	0.0005 ± 0.0005	0.0420 ± 0.001
[30]	Cal-A	fission neutrons	0.49 MeV**	0, 1, 1.7, 3.8	NR	0.059 ± 0.003
[31]	Cal-A	Am-241	2.7 MeV**	0, 0.05, 0.1, 0.2, 0.5, 0.7, 1, 1.5, 2, 2.5	NR	0.017 ± 0.002

Cal-A: calyculin A. OA: okadaic acid. NR: not reported. LINAC: linear accelerator (X-rays). Co-60: Cobalt-60 (gamma rays). Cs-137: Cesium-137 (gamma rays). Am-241: Americium-241 (alpha particles). *peak (nominal) energy. **, mean energy. SE: standard error.

To validate the curve, an estimation for an unknown dose was conducted. A sample was irradiated homogeneously at 6 Gy, with the irradiation and lymphocyte culture conditions for the unknown sample being identical to those used to generate the calibration curve. The results of this procedure are summarized in Table 4.

Table 4: Estimation of the delivered dose.

Dose delivered (Gy)	Analyzed cells	Chromosome rings	Rings per cell	Variance/mean	u Test	Estimated Dose (Gy)	Lower confidence interval (95%)	Upper confidence interval (95 %)	z score
6.0	506	80	0.16	1.294 +/- 0.063	4.708	5.651 ± 0.636	4.405 Gy	6.898 Gy	-0.8725

The delivered dose was compared to the estimated dose using the calibration curve. The acceptance criterion for the estimated dose was to fall within 20% of the delivered dose range. The z-score value was also required to be greater than -3 and less than 3.

This study illustrates the incorporation of a semi-automated analysis of PCCr spreads in the development of a dose-effect curve for X-rays. However, advancing towards fully automated analysis of PCCr spreads is achievable through the utilization of a classifier training approach, particularly with advanced automated microscopy systems. This methodology plays a crucial role in accelerating the meticulous scoring of the biomarker of interest, with resulting data systematically recorded within a customized electronic scoring sheet. The automated identification of various PCCr endpoints, alongside chromosomal rings, holds significant promise in advancing and standardizing the PCCr assay, providing essential support for enhanced precision and methodological consistency.

Numerous biodosimetric studies using the PCCr assay consistently highlight fluctuations in the α coefficient, even when subjected to comparable experimental conditions and persisting across experimental series. Notably, instances of similarity are observed, despite the use of different chemical inductors. These nuanced findings highlight the inherent complexity and variability within the PCCr assay, stressing the importance of a comprehensive understanding and meticulous interpretation of results. This is especially crucial considering the diverse experimental conditions and types of radiation employed in these studies.

4. CONCLUSIONS

After analyzing the dose-effect curve, we concluded that the frequency of chromosome rings increases linearly with the absorbed dose. A Poisson regression model ideally expects a dispersion equal to 1. In the present study, most data points follow a Poisson distribution.

The curve validation involved estimating an unknown dose, which was found to be 5.651 ± 0.636 Gy. The delivered dose was 6 Gy, with a z score of less than 3, indicating no significant difference between the estimated and delivered doses. This demonstrates that PCCr is a dependable biodosimetry tool, as chromosome rings are an appropriate indicator of high-dose radiation exposure. Moreover, obtaining enough metaphases for analysis through the conventional DCA at such high doses is impossible. In the event of a radiation incident, the expenses associated with conducting necessary PCCr tests are within reasonable and feasible limits.

Costa Rica participated in intercomparison exercises within LBDNet. Preliminary results, which demonstrate good laboratory performance, ratify adequate qualification of INISA observers. Besides this work shows that the CyberKnife® Robotic Radiosurgery system is a reliable tool for the irradiation of peripheral blood samples for X-ray biodosimetry assays and is the first time that this equipment is applied for this purpose.

ACKNOWLEDGEMENTS

The authors would like to express their gratitude to the Robotic Radiosurgery Center, which is a key institution in cancer care in Costa Rica and a valuable partner of the INISA. We are grateful for their support in developing biodosimetry and radiation biology research. We also want to acknowledge Luisa Valle-Bourrouet and Isabel Castro Volio (R.I.P.), pioneers in radiation biology research in Costa Rica.

FUNDING

This research was made possible through the financial support of the Vice-Rectorate of Research at the University of Costa Rica and the International Atomic Energy Agency.

The latter institution donated some of the necessary reagents and the Metasystems Metafer automated microscopy equipment.

CONFLICT OF INTEREST

The authors declare that they have no known competing financial interests or personal relationships that could have appeared to influence the work reported in this paper.

REFERENCES

- [1] GARCÍA, O. *ET AL.*, “The BioDoseNet image repository used as a training tool for the dicentric assay”, *Int J Radiat Biol*, vol. 95, n° 12, p. 1659–1667, 2019, doi: <https://doi.org/10.1080/09553002.2019.1665211>.
- [2] GOTOH, E., “G2 Premature Chromosome Condensation/Chromosome Aberration Assay: Drug-Induced Premature Chromosome Condensation (PCC) Protocols and Cytogenetic Approaches in Mitotic Chromosome and Interphase Chromatin for Radiation Biology”, 2019, p. 47–60. doi: 10.1007/978-1-4939-9432-8_6.
- [3] NAIRY, R. K. *ET AL.*, “Standardization of CalyculinA induced PCC assay and its advantages over Okadaic acid PCC assay in Biodosimetry applications”, *J Occup Health*, vol. 58, n° 6, p. 563–569, nov. 2016, doi: 10.1539/joh.16-0049-OA.
- [4] GUERRERO-CARBAJAL, C., I. ROMERO-AGUILERA, C. ARCEO-MALDONADO, J. E. GONZALEZ-MESA, G. E. CORTINA-RAMIREZ, e O. GARCIA-LIMA, “Dose response of prematurely condensed chromosome rings after gamma irradiation”, *Int J Radiat Biol*, vol. 95, n° 5, p. 607–610, maio 2019, doi: 10.1080/09553002.2019.1566677.
- [5] INTERNATIONAL ATOMIC ENERGY AGENCY, “Cytogenetic Dosimetry: Applications in Preparedness for and Response to Radiation Emergencies”, Vienna, 2011. [Online]. Disponível em: <http://www-ns.iaea.org/standards/>
- [6] HATZI, V. I., G. I. TERZOUDI, C. PARASKEVOPOULOU, V. MAKROPOULOS, D. P. MATTHOPOULOS, e G. E. PANTELIAS, “The use of premature chromosome condensation to study the influence of environmental factors on human genetic material in interphase cells”, *ScientificWorldJournal*, vol. 6, p. 1174–1190, 2006, doi: 10.1100/tsw.2006.210.

- [7] CORNFORTH, M. N., S. BEDFORD, e S. M. BAILEY, “Destabilizing Effects of Ionizing Radiation on Chromosomes : Sizing up the Damage”, p. 328–351, 2021, doi: 10.1159/000516523.
- [8] SISHC, B. J., C. B. NELSON, M. J. MCKENNA, C. L. R. BATTAGLIA, e C. TANZARELLA, “Telomeres and Telomerase in the radiation response : implications for instability , reprograming , and carcinogenesis”, *Front Oncol*, vol. 5, p. 1–19, 2015, doi: 10.3389/fonc.2015.00257.
- [9] MURNANE, J. P., “Telomere dysfunction and chromosome instability”, *Mutat Res.*, vol. 730, n° 415, p. 28–36, 2013, doi: 10.1016/j.mrfmmm.2011.04.008.Telomere.
- [10] XIAO, C., N. HE, Y. LIU, Y. WANG, e Q. LIU, “Research progress on biodosimeters of ionizing radiation damage”, *Radiat Med Prot*, vol. 1, n° 3, p. 127–132, set. 2020, doi: 10.1016/j.radmp.2020.06.002.
- [11] INTERNATIONAL ATOMIC ENERGY AGENCY, “Dosimetry of Small Static Fields Used in External Beam Radiotherapy An International Code of Practice for Reference and Relative Dose Determination”, Vienna, 2017.
- [12] DIETERICH, S. *ET AL.*, “Report of AAPM TG 135: Quality assurance for robotic radiosurgery”, *Med Phys*, vol. 38, n° 6Part1, p. 2914–2936, maio 2011, doi: 10.1118/1.3579139.
- [13] MISZCZYK, J., “Investigation of dna damage and cell-cycle distribution in human peripheral blood lymphocytes under exposure to high doses of proton radiotherapy”, *Biology (Basel)*, vol. 10, n° 2, p. 1–16, 2021, doi: 10.3390/biology10020111.
- [14] RADL, A., M. TAJA, C. SAPIENZA, R. BUBNIAK, M. DEMINGE, e M. GIORGIO, “Biodosimetría para sobreexposiciones con altas dosis , utilizando condensación prematura de cromosomas (PCC) químicamente inducida”, em *IX Congreso Regional de Seguridad Radiológica y Nuclear*, 2013.
- [15] HERNÁNDEZ, A. *ET AL.*, “Biodose Tools: an R shiny application for biological dosimetry”, *Int J Radiat Biol*, vol. 99, n° 9, p. 1378–1390, set. 2023, doi: 10.1080/09553002.2023.2176564.
- [16] GARCÍA, O. *ET AL.*, “The BioDoseNet image repository used as a training tool for the dicentric assay”, *Int J Radiat Biol*, vol. 95, n° 12, p. 1659–1667, dez. 2019, doi: 10.1080/09553002.2019.1665211.
- [17] GARCIA, O. F. *ET AL.*, “Intercomparison in cytogenetic dosimetry among five laboratories from Latin America”, *Mutation Research/Fundamental and Molecular*

Mechanisms of Mutagenesis, vol. 327, n° 1–2, p. 33–39, mar. 1995, doi: 10.1016/0027-5107(94)00066-E.

- [18] LLOYD, D. C. *ET AL.*, “A collaborative exercise on cytogenetic dosimetry for simulated whole and partial body accidental irradiation”, *Mutation Research/Fundamental and Molecular Mechanisms of Mutagenesis*, vol. 179, n° 2, p. 197–208, ago. 1987, doi: 10.1016/0027-5107(87)90310-1.
- [19] MIURA, T. e W. F. BLAKELY, “Optimization of calyculin A-induced premature chromosome condensation assay for chromosome aberration studies”, *Cytometry Part A*, vol. 79A, n° 12, p. 1016–1022, dez. 2011, doi: 10.1002/cyto.a.21154.
- [20] INTERNATIONAL COMMISSION ON RADIOLOGICAL PROTECTION, “The 2007 Recommendations of the International Commission on Radiological Protection”, 2007.
- [21] ROY, L. *ET AL.*, “International intercomparison for criticality dosimetry: the case of biological dosimetry”, *Radiat Prot Dosimetry*, vol. 110, n° 1–4, p. 471–476, ago. 2004, doi: 10.1093/rpd/nch349.
- [22] MEENAKSHI, C., P. VENKATACHALAM, S. CHANDRASEKARAN, e B. VENKATRAMAN, “Construction of dose response curve for 6 MV LINAC X-rays using Premature Chromosome Condensation assay for radiation dosimetry”, *Applied Radiation and Isotopes*, vol. 173, p. 109729, jul. 2021, doi: 10.1016/j.apradiso.2021.109729.
- [23] LAMADRID, A., O. GARCÍA, M. DELBOS, P. VOISIN, e L. ROY, “PCC-ring induction in human lymphocytes exposed to gamma and neutron irradiation”, *J Radiat Res*, vol. 48, n° 1, p. 1–6, 2007, doi: 10.1269/jrr.0625.
- [24] PUIG, R., L. BARRIOS, M. PUJOL, M. R. CABALLÍN, e J.-F. BARQUINERO, “Suitability of scoring PCC rings and fragments for dose assessment after high-dose exposures to ionizing radiation”, *Mutation Research/Genetic Toxicology and Environmental Mutagenesis*, vol. 757, n° 1, p. 1–7, set. 2013, doi: 10.1016/j.mrgentox.2013.03.013.
- [25] ROMERO, I. *ET AL.*, “Assessment of simulated high-dose partial-body irradiation by PCC-R assay”, *J Radiat Res*, vol. 54, n° 5, p. 863–871, set. 2013, doi: 10.1093/jrr/rrt032.
- [26] ROMERO, I., A. I. LAMADRID, J. E. GONZÁLEZ, T. MANDINA, e O. GARCÍA, “Culture time and reagent minimization in the chemical PCC assay”, *Int J Radiat Biol*, vol. 92, n° 10, p. 558–562, 2016, doi: 10.1080/09553002.2016.1206236.
- [27] SUN, M., J. MOQUET, S. BARNARD, D. LLOYD, e E. AINSBURY, “A Simplified Calyculin A-Induced Premature Chromosome Condensation (PCC) Protocol for the

Biodosimetric Analysis of High-Dose Exposure to Gamma Radiation”, *Radiat Res*, vol. 193, n° 6, p. 560, mar. 2020, doi: 10.1667/RR15538.1.

- [28] BALAKRISHNAN, S., KAPIL SHIRSATH, N. BHAT, e K. ANJARIA, “Biodosimetry for high dose accidental exposures by drug induced premature chromosome condensation (PCC) assay”, *Mutation Research/Genetic Toxicology and Environmental Mutagenesis*, vol. 699, n° 1–2, p. 11–16, jun. 2010, doi: 10.1016/j.mrgentox.2010.03.008.
- [29] LINDHOLM, C. *ET AL.*, “Premature Chromosome Condensation (PCC) Assay for Dose Assessment in Mass Casualty Accidents”, *Radiat Res*, vol. 173, n° 1, p. 71–78, jan. 2010, doi: 10.1667/RR1843.1.
- [30] LAMADRID, A. I., J. E. GONZÁLEZ, O. GARCÍA, P. VOISIN, e L. ROY, “Prematurely Condensed Chromosome Rings after Neutron Irradiation of Human Lymphocytes”, *J Radiat Res*, vol. 52, n° 4, p. 531–535, 2011, doi: 10.1269/jrr.10096.
- [31] PUIG, R., M. PUJOL, L. BARRIOS, M. R. CABALLÍN, e J.-F. BARQUINERO, “Analysis of α -particle-induced chromosomal aberrations by chemically-induced PCC. Elaboration of dose-effect curves”, *Int J Radiat Biol*, vol. 92, n° 9, p. 493–501, set. 2016, doi: 10.1080/09553002.2016.1206238.
-

LICENSE

This article is licensed under a Creative Commons Attribution 4.0 International License, which permits use, sharing, adaptation, distribution and reproduction in any medium or format, as long as you give appropriate credit to the original author(s) and the source, provide a link to the Creative Commons license, and indicate if changes were made. The images or other third-party material in this article are included in the article’s Creative Commons license unless indicated otherwise in a credit line to the material. To view a copy of this license, visit <http://creativecommons.org/licenses/by/4.0/>.